Depositional characteristics and trace metal abundance of sediments in an anoxic basin

Trevor Harrison

University of Washington, School of Oceanography

Advisor: Julian Sachs

Acknowledgements

I would like to thank Julian Sachs, Arthur Nowell, Ashley Maloney, and Kathy Newell for their continual guidance, support, and patience while conducting this study. I would also like to thank Julia Marks, Colton Skavicus, and Caroline Bellman for contributing to certain data analyses and constructive input. Additionally, I would like to thank Michelle Harrison for her contributions to this study.

Abstract

Radiocarbon dates, grain-size analysis, $\delta^{13}C$, Computerized Tomography Scans, and metal abundance profiles are used to identify sediment deposition rate, sediment source, and redox conditions in a basin cut off from deep water renewal by a sill on the western coast of Vancouver Island B.C. Coarse silt is deposited at a rate of 0.5cm yr^{-1} in seasonally varying laminations preserved by anoxic conditions. Dark, organic rich laminations have heavier $\delta^{13}C$ ratio than adjacent light bands indicating some source of C4 organic matter. Trace metal profiles reveal a long history of anoxic conditions, but a homogenized surface sediment layer and redox sensitive profiles indicate the possibility of a recent bottom oxygenation event.

Introduction

Muchalat Inlet is one of many long, narrow, steep-sided fjords carved into the western coast of Vancouver Island B.C. during the Last Glacial Maximum 17 kya(Dodimead 1984; Milliman and Syvitski 1992; Nuwer and Keil 2005). It's anoxic basin, cut off from deep water renewal by a shallow sill at the inlet's mouth, is a site of net sediment accumulation and a sink for terrigenous organic carbon (TOC) (Pickard 1963; Milliman and Syvitski 1992; Calvert and Pedersen 1993; Nuwer and Keil 2005). TOC and trace metals adsorbed onto the surface of sediments are delivered into this reservoir via non-point source debris flows and riverine input at the head of the fjord (Walsh et al. 2008). While massive amounts of coarse grained sediments such as gravel and sand can be instantaneously deposited in these non-point source events, rivers are the main source of the fine grained sediments the majority of TOC and trace metals are bound to due to their large surface areas and ideal cation exchange capacity (Horowitz 1985; Hedges and Keil 1995). These fine sediments have the potential to be deposited in unperturbed laminations due, in part to, the lack of macro benthic communities in the anoxic basin (Calvert and Pedersen 1993). Besides riverine and non-point source flows, changes in the concentration of trace msetals in TOC-rich sediments is due to the deposition of marine organic matter like planktonic remains and early diagenetic enrichment (Brumsack 2006). Differentiating between these sources is difficult but necessary to gain an understanding of the historical record of chemical conditions, contaminate input, and background concentrations of trace metals.

This goal of this study is to measure the general depositional characteristics and trace metal abundance in sediments from the basin of Muchalat Inlet in Vancouver B.C. To do this I will answer these questions: What is the sedimentation rate? What grain size are the particles being

deposited? Are the sediments terrestrially or marine derived? Is there any seasonal variation? What are the trace metal abundances in the sediments? Are there any trends in trace metal profiles?

To answer these questions, I will use grain size analysis, radiocarbon dating, $\Delta^{13}C$ analysis to determine the source of sediments, test for metal abundance, and use CT scans.

Methods

Field Sampling

This study was primarily conducted in Muchalat Inlet, Vancouver Island B.C. onboard the R/V *Thompson* on 11-21 December, 2014. Sediment cores were collected from station M04a at an approximate depth of 347m using a 60cm long, spade arm box corer (20cm x 30cm cross-sectional area) and a 180cm long Kasten corer (12cm x 12cm cross-sectional area) (Figure 1).

Figure 1. Map of Muchalat Inlet in Nootka Sound, Vancouver B.C. M04a Core site marked on map. *Map curtesy of Julia Marks

Samples were taken from the box core using a 60cm barrel (internal diameter ~4in) and a 60cm (10cm x 2cm cross-sectional area) X-ray tray. The X-ray tray was capped and stored vertically at ~4°C until ready for imaging. The sediments in core barrel were extruded onboard the ship into polyethylene whirlpack bags in 1cm increments for the top 10cm, and 2cm increments for the remainder of the core using metal spatulas. These bags were stored at ~4°C.

Upon the Kasten corer's retrieval, a neoprene pad was inserted at the top of the barrel to stop slumping. The corer was then laid horizontally and opened. The first 29cm of sub-surface sediments were impossible to section due to their high water content so they were collected and homogenized in a large zip-lock bag. Starting at 29cm below the top and continuing down the length of the core barrel, 30cm long X-ray trays (2cm x 10cm cross-sectional area) were pushed into the exposed sediments. The fourth side of the trays were slid into place and each tray was removed from the barrel and stored with the other X-ray trays. The remaining sediments in the core were sectioned, 1cm increments between 29-59cm and 2cm increments for the remainder, using metal plates and placed into the same sample bags using metal spatulas.

Sediments used for surface $\delta^{13}C$ analysis were collected in Tahsis Inlet and at other stations in Muchalat with the box corer using the same procedures.

It is important to note that, due to the over-penetration of the box corer and Kasten corer in Muchalat Inlet, surface sediments were not captured in the core barrels. Despite the over-penetration, surface interface was preserved above the upper limits of the actual box being used as evident by a thin film of sulfur-reducing bacteria found on the sediments. This surface layer was preserved and stored in a separate sample bag.

The X-ray trays taken from the box core and Kasten core at M04a were scanned using a Siemens biograph 16 CT scanner at Via Radiology in Seattle, WA. The high resolution X-ray images provided by these scans show changes in density throughout the core. These images were examined and manipulated using the syngo Media Viewer software provided by Siemans.

X-ray Tray Sub Sampling

Sediments collected in the X-ray trays from the M04a box core and the M04a Kasten core (29cm-59cm) were subsampled and used for grain size analysis, heavy metal analysis, organic carbon analysis, and $\delta^{13}C$ analysis. Subsamples were chosen based off of alternating light and dark laminations that corresponded with changes in density shown in the CT scans. The X-ray trays were opened by sliding the lid vertically out of the tray. Sediment was collected using a variety of metal spatulas and sampling needles.

Radiocarbon Dating

Organic material used for Carbon 14 dating was collected from both cores taken at station M04a. Sediments were taken from depths of 12-14cm and 18-20cm in the box core and from depths of 40-41cm, 45-46cm, and 50-51cm in the Kasten core, and sieved for terrestrial macrofossils. Approximately 0.5-2mg of organic material was collected from each depth and ran through an Acid-Base-Acid treatment established by (Brock et al. 2010). After treatment, the samples were sent to DirectAMS in Bothell, WA for radiocarbon analysis using National Electrostatics Corporation 1.5SDH-1 Pelletron Accelerator. The results, reported in $F^{14}C$, were calibrated for age using the ^{14}Chrono Centre from Queen's University Belfast (http://www.calib.qub.ac.uk/CALIBomb/).

Grain Size Analysis

Homogenized samples, weighing between 20-30g, were treated with 15mL of 30% H_2O_2 and heated at 60°C for 3-4 hours. Samples were then wet sieved through a 62 µm sieve to separate silts and clays from coarser particles. Material with a diameter greater than 62 µm (-4φ), or the coarse fraction, is dried and shaken through a nest of sieves in 0.5φ increments from -4φ to 4φ in a Ro-Tap for 15 minutes. Material with a diameter of less than 62 µm were analyzed using the pipette method outlined in (King 1978). The mass data for each size fraction of each sample was processed using GRADISTAT (Blott and Pye 2001).

Metals and Organic Carbon Content

Samples of dried, crushed, sediments were submitted to Dongsen Xue, manager of the Analytical Service Center in the School of Environment and Forest Sciences at the University of Washington, to test for metals abundance. Samples were digested using the EPA 3050B method (1996) and tested for metals abundance using a model 61E Thermo Scientific ICP-AES instrument.

After the samples were returned, organic carbon content was evaluated by Julia Marks of the University of Washington by means of measuring loss on ignition. Each sample was weighed, combusted at 400°C for 12 hours, and weighed again. The mass loss on ignition was used as a proxy for %OC (Schumacher 2002). Samples were dried at a temperature of 140°C prior to the metals analysis, possibly resulting in a loss of extremely volatile carbon.

The metals and organic carbon data were analyzed using Principal Component Analysis (PCA). The data was standardized to the standard deviation of the concentration of each metal down-core. The analysis was run in PC-ORD 5.0 using the Variance/Covariance (centered) option in variables space (McCune and Mefford 2011).

To determine whether metal concentrations deviated from their natural abundance, the ratios of individual metals to Al occurring in each sample were compared to the same ratios in organic rich shale using the equation:

$$EF = (element/Al)_{Sample}/(element/Al)_{Shale}^{a} \quad (1)$$

Due to its crustal abundance, stability, and insignificant input from other sources, aluminum is often used to compare metal concentrations to their own average crustal abundance and to other metals (Wedepohl 1971; Horowitz 1985; Schropp and Windom 1988). Metals with an enrichment factor (EF) >1 are enriched relative to their natural abundance while metals with an EF <1 are depleted. This is an important tool in identifying contaminates and determining the redox conditions in bottom waters and deep basin sediments at the time of deposition (Huang and Lin 2003; Brumsack 2006).

$\delta^{13}C$

Samples were prepared for carbon isotope analysis by placing 5-100mg of dried sediment into a pressed tin cup and treated with 2 N HCl until effervescence ceased as described in (Sachs and Repeta 2000). Samples were sent to the Stable Isotope Facility in the Department of Plant Sciences at the University of California Davis and analyzed for ^{13}C isotopes using an Elementar Vario EL Cube or Micro Cube elemental analyzer (Elementar Analysen systeme GmbH, Hanau, Germany) interfaced to a PDZ Europa 20-20 isotope ratio mass spectrometer (Sercon Ltd., Cheshire, UK). Procedures for this analysis can be found at (http://stableisotopefacility.ucdavis.edu).

Results

Computerized Tomography Scan

Darker shades represent lower density materials while lighter shades denote the opposite. Both cores contain the same pattern of well-defined laminations occurring between 8 and 42cm beneath the mud's surface (Figure 2).

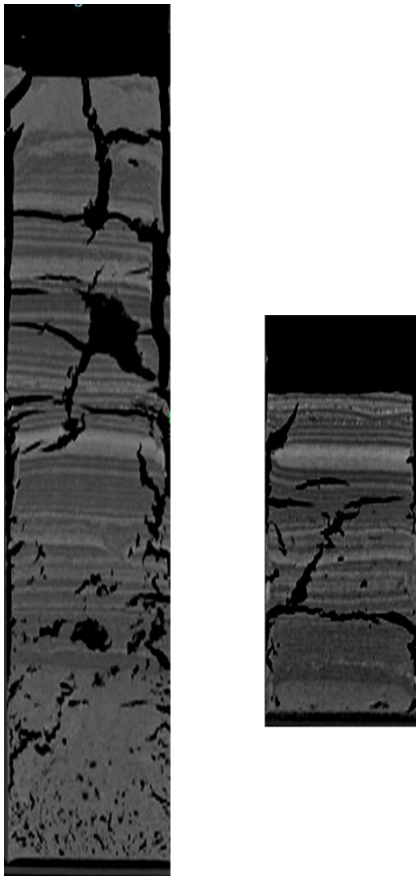

Figure 2. CT scan images of M04a box core 0-60cm (left) and Kasten core 29-59cm (right) aligned by corresponding laminations

Radiocarbon Dating

Possible radiocarbon dates estimated from two depths in the box core and three depths from the Kasten core taken at station M04a are plotted on (Fig.3 a, Fig.3b). A linear regression line was fit to the most probable dates for each core (Fig.3c, Fig3. d). The box core showed sediments at 13cm and 19cm were deposited in 1987 and 1975, respectively. The Kasten core showed sediments at depths of 30cm and 40cm were deposited in 1978 and 1959, respectively. The dates estimated from the sample taken at 45cm from the Kasten core showed an age reversal and were not used in the linier regression. Both cores revealed sediments were deposited at approximately 0.5cm yr^{-1}

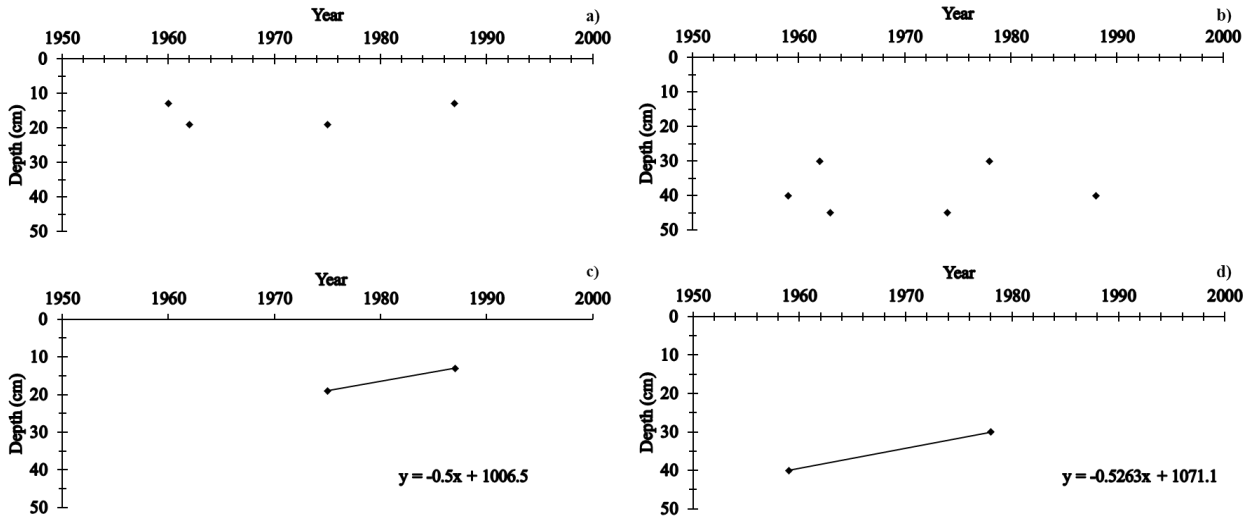

Figure 3. Four profiles of radiocarbon dates from two cores. 3a) and 3c) are the estimated radiocarbon dates from the box core and estimated deposition rate based on the dates with the highest probabilities, respectively. 3b) and 3d) corresponding plots from the Kasten core.

Varves

The sedimentation rate of 0.5cm yr^{-1} was applied to the length of the box core to determine if pairs of laminations were being deposited annually. Biannually deposited layers, or varves, are help identify seasonal changes in depositional regimes. Distinct layers were counted in five 3cm long sections throughout the core using the syngo Media Viewer software provided by Siemans. If biannual deposition were occurring, there would be an average of 12 laminations per 3cm section, or 4 laminations per 1cm (Table 1). The average number of laminations in each 3cm section was 10.6, or 3.5 laminations per cm proving that varves were being deposited.

Table 1. Expected # of laminations based on deposition rate calculated from radiocarbon dates. Measured layers were counted using the syngo Media Viewer software provided by Siemans.

Section	Sample Length (cm)	Expected # of Layers	Measured # of Layers
A	3	12	11
B	3	12	9
C	3	12	12
D	3	12	9
E	3	12	12
Average	**1**	**4**	**3.53**

Grain Size Analysis

The mean grain size of four samples from different depths in the laminated portion of the box core ranged from 4.655φ to 6.617φ classifying the sediments as medium to coarse silts (Figure 4). Samples a) and b) were from a high density lamination and both contained small amounts of gravel and sand (Fig.4 a,b). Sample c) contained sediments from a mix of high and low density bands, while sample d) was composed only of low density material (Fig.4 c,d). Both samples contained a relatively larger portion of sand by weight and were classified in the textural group "sandy mud" by GRADISTAT. All samples contained a wide spectrum of grain sizes.

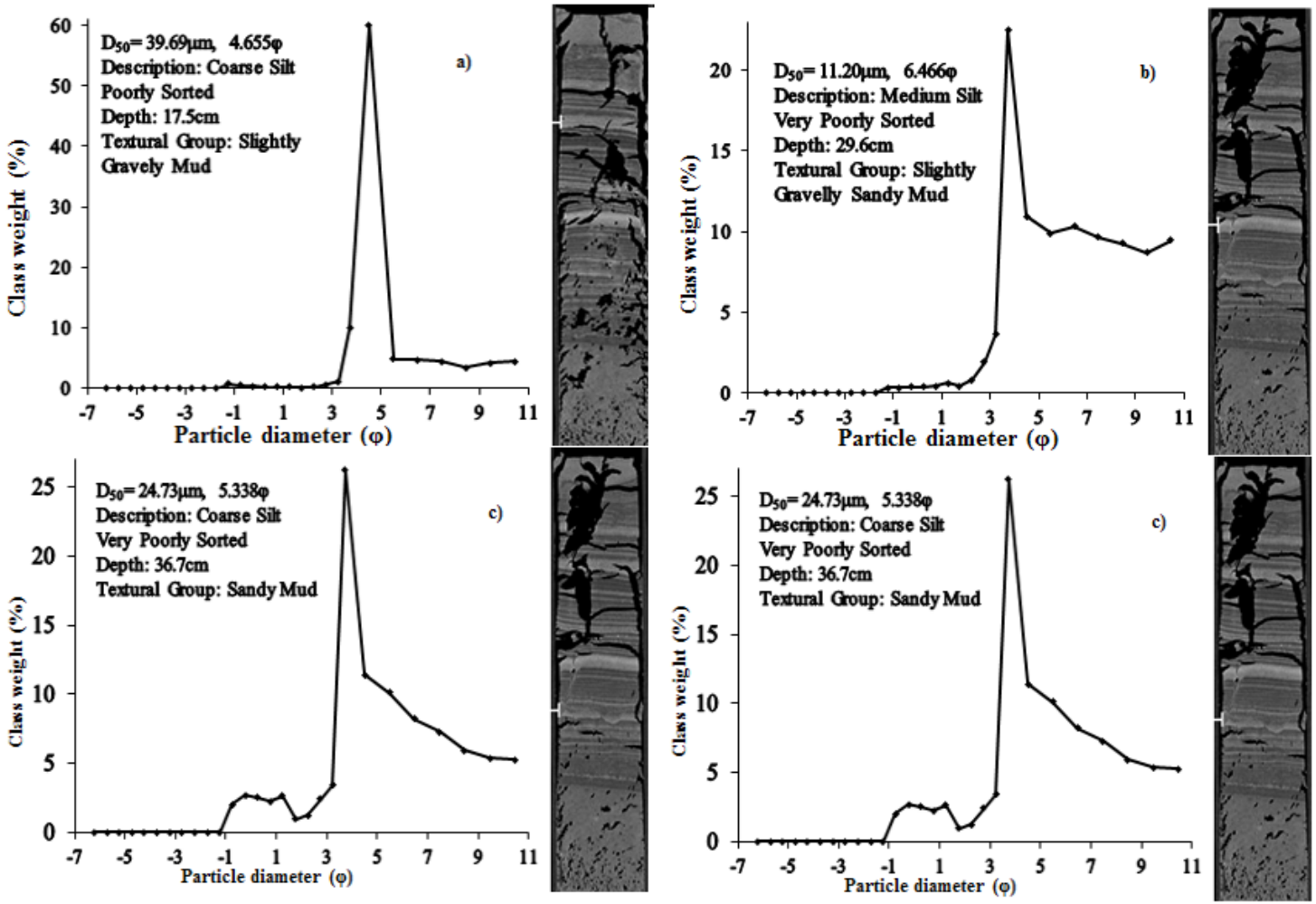

Figure 4. Grain size distributions from four samples taken from M04a box core. 4a) is sampled from a light band at 17.5cm. 4b) is from a light band at 29.6cm. 4c) is from a combination of light and dark sediments at 36.7cm. 4d) is from a dark band at 42.9cm

Table 2. Element/Al ratios and %OC values of sediments taken from Muchalat inlet. Discriptions of the laminations sediments were sampled from included. Massive = Homogeneous

Layer Color	Depth (cm)	Ag/Al	B/Al	Ba/Al	Ca/Al	Cd/Al	Cr/Al	Cu/Al	Fe/Al	K/Al	Mg/Al	Mn/Al	Mo/Al	Na/Al	Ni/Al	P/Al	Pb/Al	S/Al	Se/Al	Si/Al	Zn/Al	%OC/Al	%OC
Massive	1	1.57E-07	0.0066	0.0066	0.007	6.6E-03	0.0066	0.0066	0.007	0.007	0.007	0.0066	0.0066	0.0066	0.0066	0.050	0.0023	0.31	0.018	0.034	0.0031	0.0006	16.1
Massive	2.5	1.57E-07	0.0095	0.0032	1.059	6.6E-03	0.0031	0.0043	1.83	0.24	0.94	0.23	0.0037	3.11	0.0037	0.061	0.0027	1.05	0.022	0.16	0.0055	0.0011	16.8
Dark	5.5	1.57E-07	0.0080	0.0025	1.035	6.6E-03	0.0031	0.0046	1.62	0.18	0.86	0.60	0.0038	2.15	0.0036	0.064	0.0026	0.69	0.022	0.20	0.0047	0.0009	15.2
Light	9.5	1.57E-07	0.0074	0.0026	0.802	6.6E-03	0.0029	0.0047	1.75	0.16	0.81	0.08	0.0037	1.89	0.0032	0.055	0.0026	0.74	0.021	0.15	0.0043	0.0009	15.7
Light	12.5	1.57E-07	0.0084	0.0026	1.151	6.6E-03	0.0031	0.0046	1.59	0.15	0.76	1.05	0.0039	1.36	0.0035	0.065	0.0017	0.69	0.023	0.058	0.0045	0.0011	19.6
L D	16.2	1.57E-07	0.0076	0.0027	0.797	6.6E-03	0.0028	0.0048	1.73	0.14	0.74	0.19	0.0036	1.27	0.0031	0.050	0.0024	0.68	0.021	0.116	0.0041	0.0009	16.9
Light	17.5	1.57E-07	0.0054	0.0017	0.596	6.6E-03	0.0023	0.0052	1.48	0.09	0.63	0.04	0.0027	0.69	0.0025	0.049	0.0023	0.31	0.018	0.021	0.0031	0.0006	13.3
Dark	20.1	1.57E-07	0.0119	0.0042	1.002	6.6E-03	0.0035	0.0048	1.86	0.21	0.88	0.06	0.0051	2.25	0.0033	0.062	0.0027	1.23	0.021	0.084	0.0051	0.0022	31.7
L D	25.4	1.57E-07	0.0075	0.0024	0.774	6.6E-03	0.0027	0.0049	1.60	0.13	0.73	0.04	0.0039	1.23	0.0027	0.053	0.0025	0.66	0.019	0.040	0.0040	N/A	N/A
Light	29.6	1.57E-07	0.0062	0.0021	0.657	6.6E-03	0.0022	0.0050	1.46	0.12	0.61	0.04	0.0029	0.86	0.0024	0.054	0.0025	0.45	0.018	0.023	0.0048	0.0006	12.8
LDL	32.8	1.57E-07	0.0090	0.0022	1.425	6.6E-03	0.0029	0.0046	1.59	0.18	0.73	0.05	0.0044	1.54	0.0031	0.062	0.0029	0.84	0.019	0.053	0.0049	0.0013	21.7
L D	36.7	1.57E-07	0.0053	0.0019	0.623	6.6E-03	0.0027	0.0048	1.59	0.13	0.65	0.04	0.0029	0.89	0.0027	0.045	0.0026	0.53	0.019	0.061	0.0039	0.0007	12.6
L D	39.8	1.57E-07	0.0068	0.0018	0.732	6.6E-03	0.0026	0.0047	1.61	0.15	0.71	0.04	0.0036	1.17	0.0028	0.047	0.0024	0.63	0.019	0.055	0.0041	0.0008	14.5
Dark	42.9	1.57E-07	0.0075	0.0018	0.809	6.6E-03	0.0040	0.0044	1.76	0.17	0.74	0.06	0.0034	1.38	0.0032	0.051	0.0027	0.75	0.021	0.049	0.0046	0.0010	16.2
Massive	48.5	1.57E-07	0.0064	0.0017	0.653	6.6E-03	0.0025	0.0049	1.61	0.13	0.72	0.04	0.0029	0.97	0.0027	0.040	0.0022	0.77	0.019	0.076	0.0034	0.0007	13.0

Metals and Organic Carbon Content

Trace metal/Al ratios, %OC/Al ratios, and %OC are reported in (Table 2). It is important to point out that LOI was not performed for the sample at 25.4cm and is represented in any figure it is included in as 0. %OC ranged from a maximum of 31.7 at 20.1cm deep to a minimum of 12.6 at a depth of 36.7cm. The high maximum value of 31.7 may be an error due to small sample size during the LOI procedure, and should be treated as such. The next highest value of 21.7 occurred at a depth of Average trace metal/Al ratios for shale and sediments from the M04a box core, along with each element's mean EF are shown in (Table 3). Ba, K, Mn, and Si are depleted and Cd and Mo have extremely high EF values compared to other enriched metals, ranging from 185-313 in Cd and 178-290 in Mo. All elements, with the exception of Ag, remain either depleted or enriched for all depths. Ag concentrations dramatically increase between 2cm-12.5cm, with EF values ranging from 197-77, and drop down to nearly undetectable amounts in the rest of the core (Table 3, Fig.7).

Table 3.Element/Al ratios of average shales compared to sediments in Muchalat Inlet. Enrichment factor (EF) >1 show an enrichment in metal concentrations in Muchalat sediments relative to their standard concentrations, values <1 show depletions. Cd and Mo are unusually enriched in these samples. Ag is the only metal that varies in enrichment/depletion down core (Fig. 7).

Element	Average Shale[a]	Muchalat Inlet	Mean EF	EF Std. Dev.
Ag/Al	8.00E-07	0.00005	65.7	108.8
Ba/Al	0.0066	0.0024	0.4	0.1
Ca/Al	0.18	0.84	4.8	1.32
Cd/Al	0.0000015	0.00037	248.4	41.1
Cr/Al	0.00102	0.0028	2.8	0.46
Cu/Al	0.00051	0.0049	9.3	0.47
Fe/Al	0.055	1.63	30.0	2.2
K/Al	0.34	0.15	0.5	0.11
Mg/Al	0.18	0.74	4.2	0.53
Mn/Al	96	0.17	0.0	0.0031
Mo/Al	0.000015	0.0035	241.0	42.9
Na/Al	0.13	1.43	11.4	5.1
Ni/Al	0.00077	0.0030	3.9	0.5
P/Al	0.008	0.0537	6.8	0.9
Pb/Al	0.00025	0.0025	10.0	1.2
Si/Al	3.11	0.079	0.0	0.017
Zn/Al	0.0011	0.0043	4.0	0.6

[a]Values taken from (Brumsack 2006), calculated from (Wedepohl 1971).

Principal component analysis revealed covariance between trace metal/aluminum ratios and %OC/Al with respect to depth (Figure 5). Plot a shows Axis 1 vs Axis 2, Plot b shows 1 vs 3, and plot c shows 2 vs 3. $\delta^{13}C$ and grain size data were not included in the analysis due to small sample sizes. Axis 1 explains 30% of variance, Axis 2 explains 25% of variance, and Axis 3 explains 15%. The first major distinction between co-varying metals is whether they are plotted as positive or negative values on Axis 1(Fig.5 a). Si, P, Ag, Mn, Pb, Cu, and %OC are plotted on the positive side of the axis, implying that their concentrations are controlled by the same factor in some capacity. Other groupings of co-varying elements include (Ba,Cr,Cd,Zn,S) (K,Fe,Na,Mg) (%OC,Mo,Ba) (Figures 6,7,8,9). Within the previously mentioned groups, the strongest co-variance exists between Mo and Ba, Zn and Cr, Na and Mg, and Ni and Se.

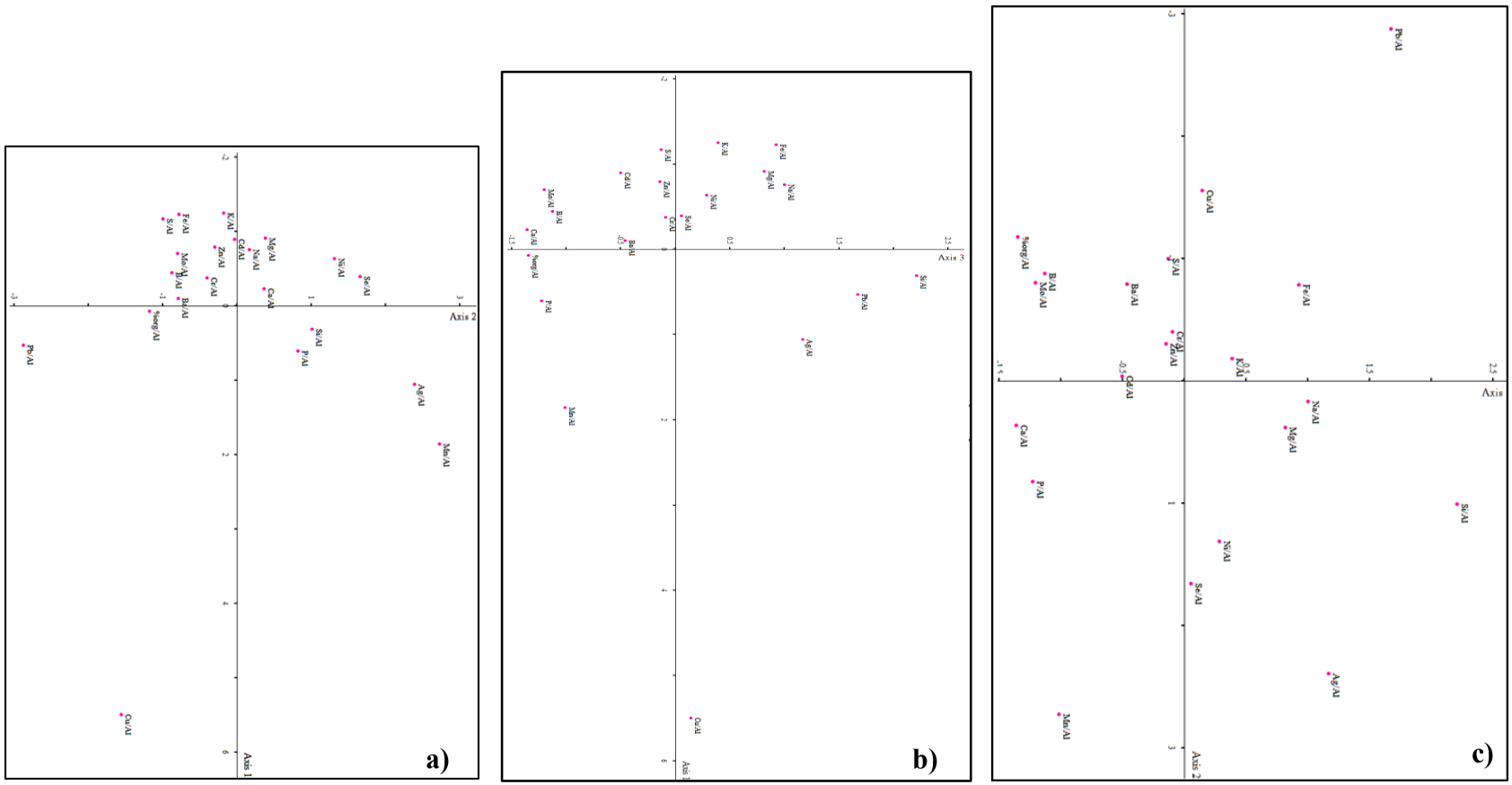

Figure 5. PCA results for elements/Al and %OC/Al. 5a) Axis 1vs2. 5b) Axis 1vs3. 5c) Axis 2vs3. Axis 1 explains 30% variance, Axis 2 explains 25%, and Axis 3 explains 15%

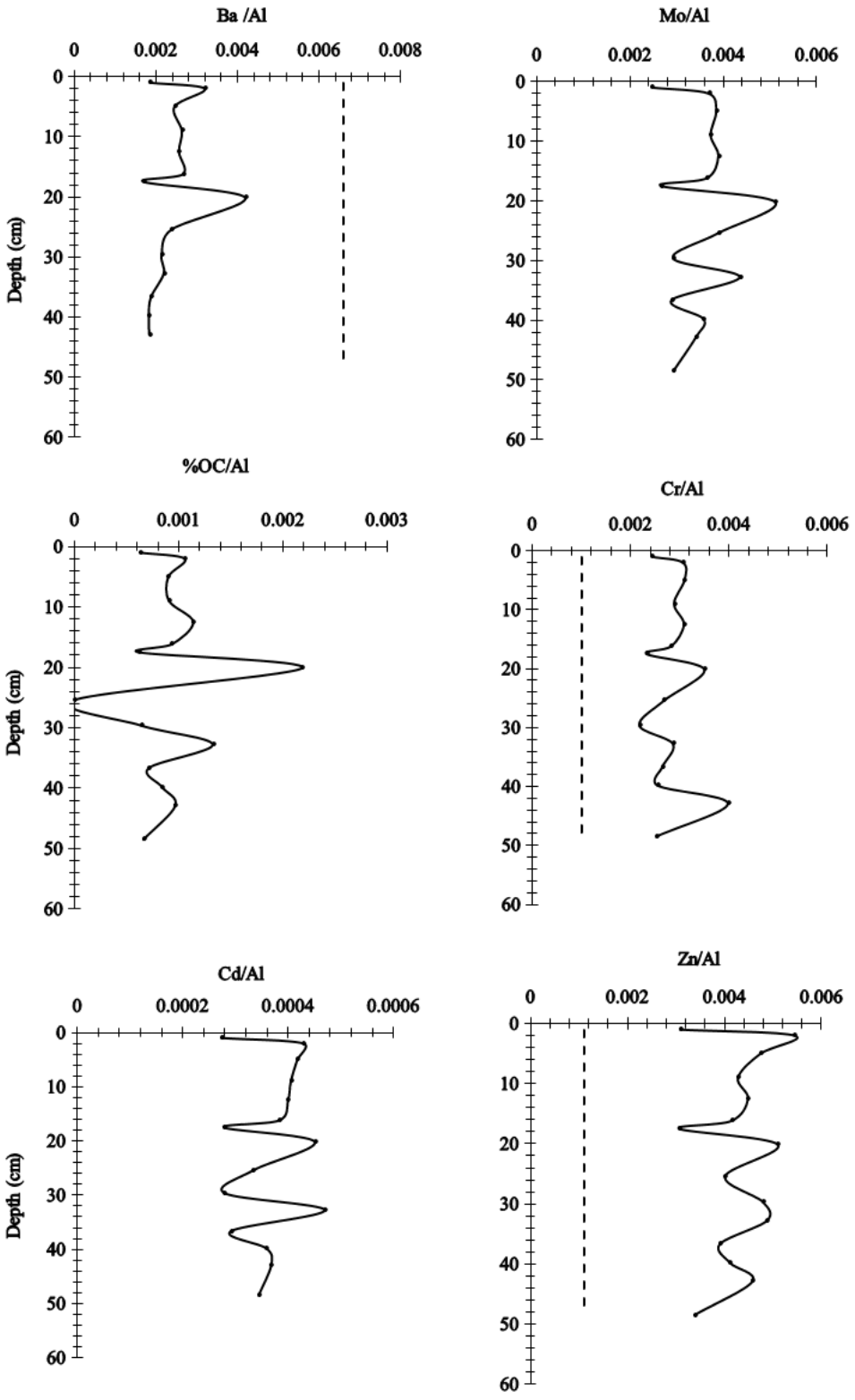

Figure 6. Plots of Ba, Mo, %OC, Cr, Cd, and Zn normalized to Al. Dashed lines represent natural abundance in shale (Wedepohl 1971).

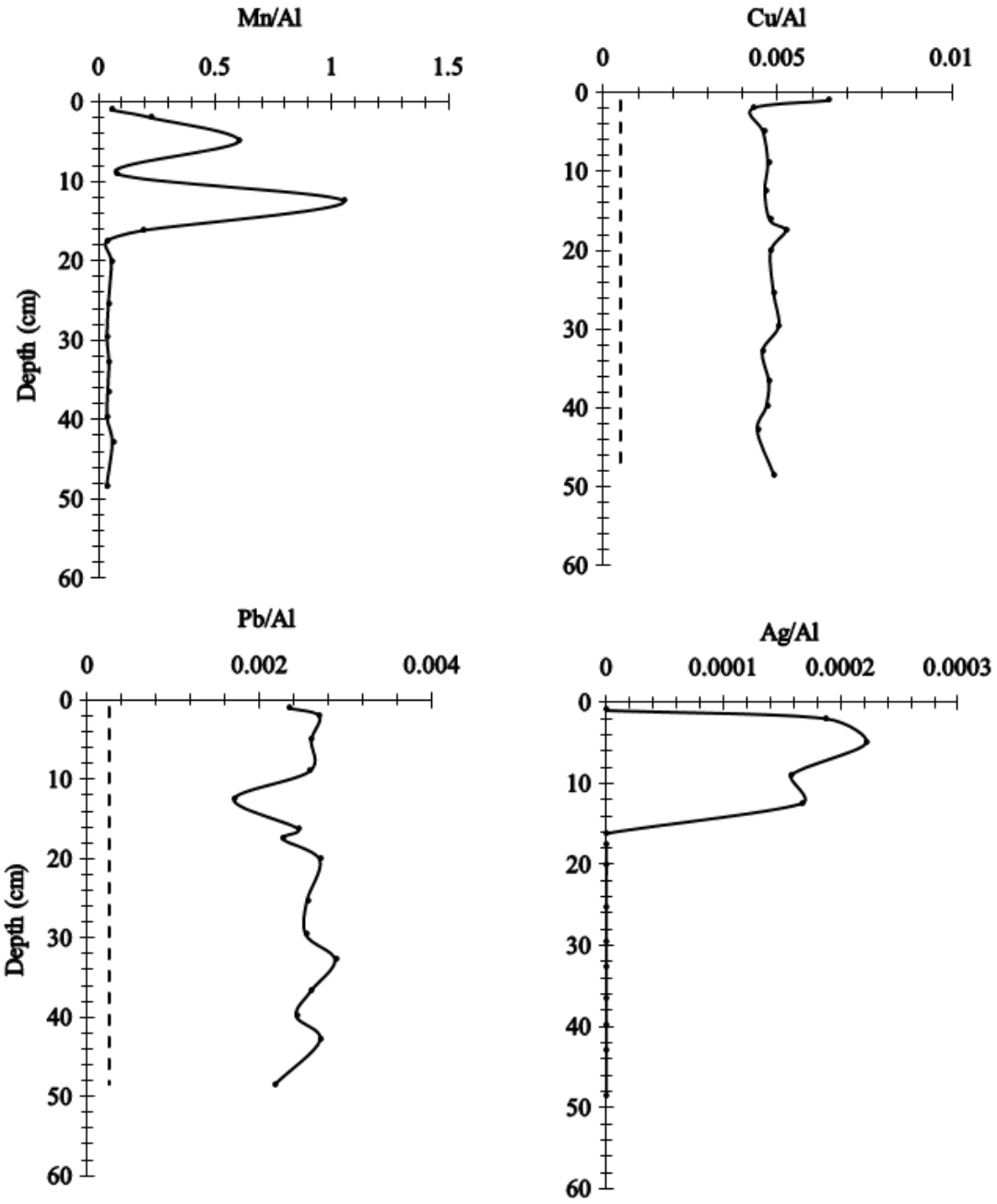

Figure 7. Plots of Mn, Cu, Pb, and Ag normalized to Al. Dashed lines represent natural abundance in shale (Wedepohl 1971).

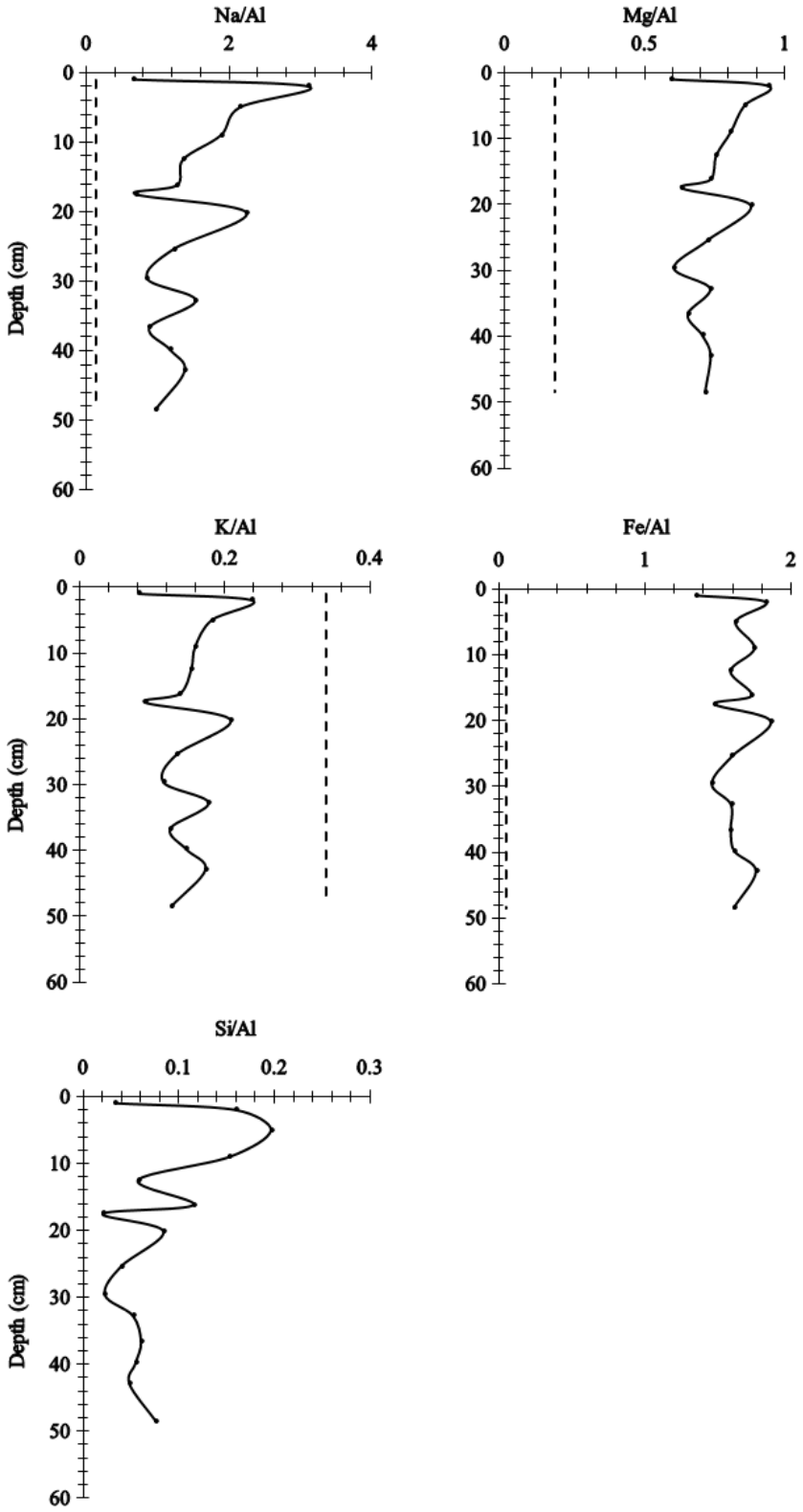

Figure 8. Plots of Na, Mg, K, Fe, Si normalized to Al. Dashed lines represent natural abundance in shale (Wedepohl 1971).

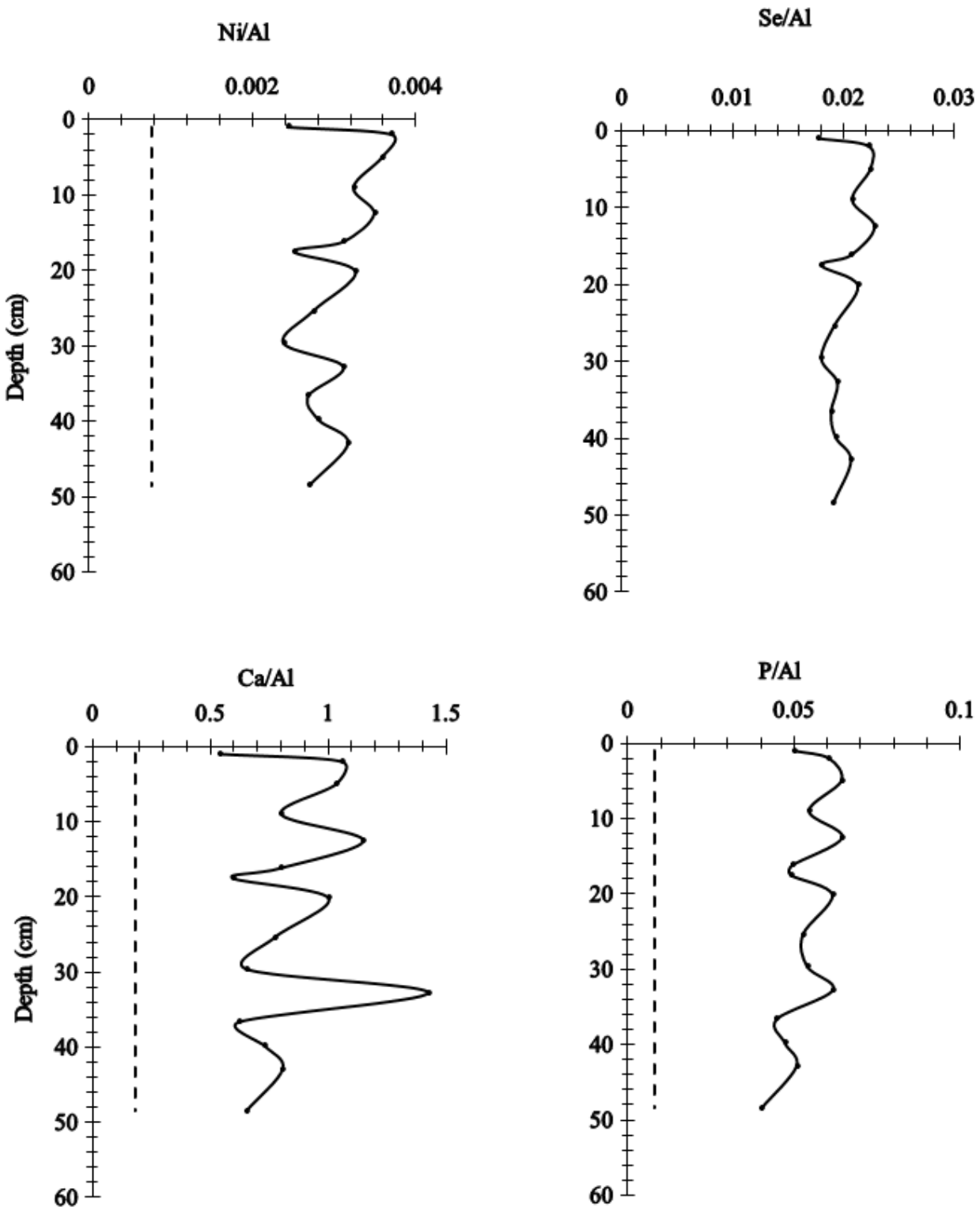

Figure 9. Plots of Ni, Se, Ca, and P normalized to Al. Dashed lines represent natural abundance in shale (Wedepohl 1971).

$\delta^{13}C$

$\delta^{13}C$ values of surface sediments taken from transects in Muchalat and Tahsis Inlets are plotted in (Figure 10). $\delta^{13}C$ ratios are lowest at the heads of both inlets indicating higher abundance of terrestrial organic carbon in the sediments, and become more positive towards their mouths, suggesting that larger amounts of marine derived organic matter is being deposited near Nootka Sound. An exception to this is seen at station T06 in Tahsis Inlet, where sediments with a more positive $\delta^{13}C$ ratio than those taken from a station closer to the mouth were deposited outside of the entrance to Hecate Channel.

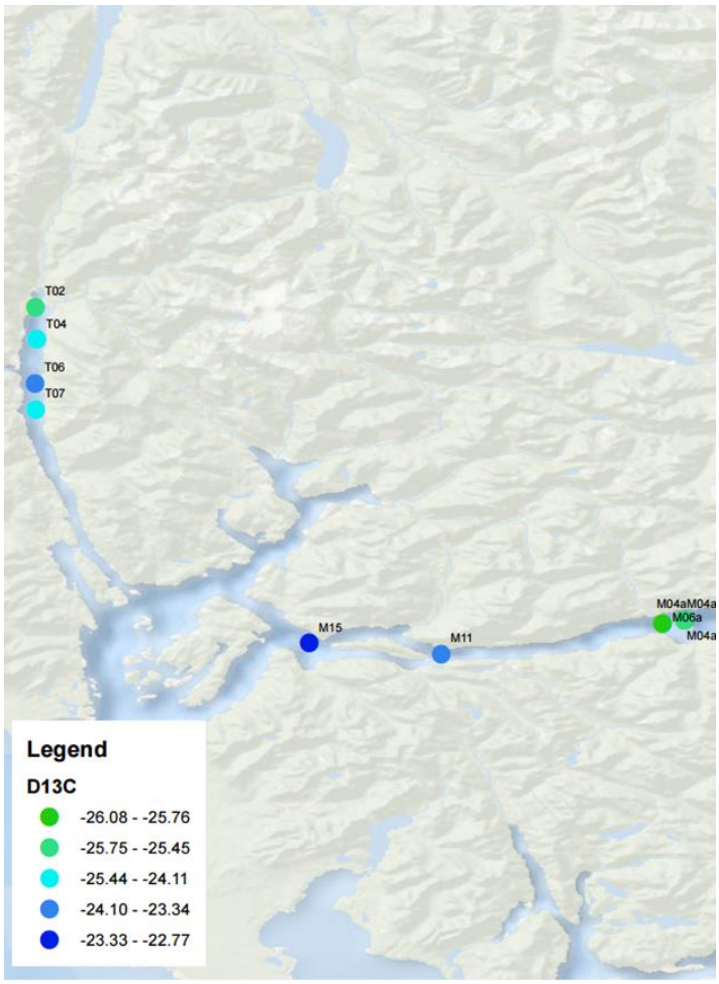

Figure 10. $\delta^{13}C$ of surface sediments in Muchalat and Tahsis Inlets.

$\delta^{13}C$ ratios of sediments from alternating light and dark bands taken from the box and Kasten core X-ray trays are shown in (Figure 11,Table 4**).** Values ranged from -27.10‰ to -24.97‰ throughout the core's entirety, and varied an average of -.47‰ between adjacent light and dark bands. Sediments from light bands, expressed as hollow points on in the figure, have more negative values than their dark counterparts represented by solid symbols. Also, samples from the box core have more negative values than samples from the Kasten core including sediments from corresponding laminae.

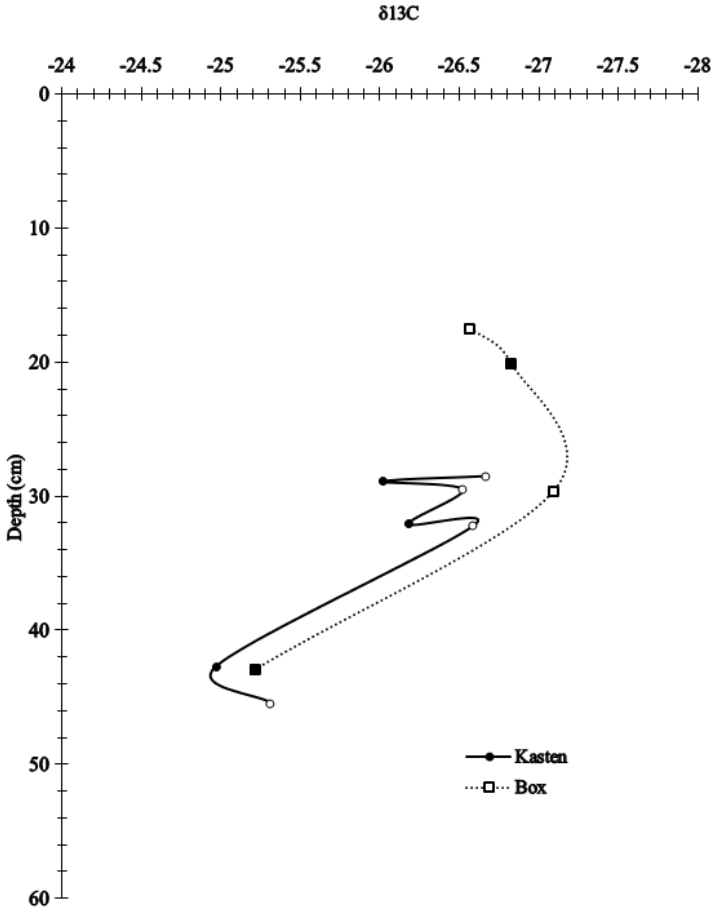

Figure 11. δ13C values of sediments down core. Filled symbols represent sediments taken from dark laminations and hollow symbols represent the opposite.

Table 4. δ13C values of sediments taken from X-ray trays from both cores. Samples from Kasten

Depth (cm)	Coring Device	δ13C	Description	C Amount (µg)	Sample Weight (µg)
17.5	Box	-26.57	Light	250.66	4919
20.1	Box	-26.83	Dark	981.82	6074
28.5	Kasten	-26.67	Light	445.71	9366
28.9	Kasten	-26.02	Dark	329.49	3404
29.5	Kasten	-26.52	Light	77.31	593
29.6	Box	-27.10	Light	162.98	4961
32.1	Kasten	-26.18	Dark	644.20	6607
32.2	Kasten	-26.59	Light	278.85	4563
42.7	Kasten	-24.97	Dark	247.84	4603
42.9	Box	-25.22	Dark	424.77	8822
45.4	Kasten	-25.32	Light	63.63	3139

Discussion

Sediment deposition

Based on the deposition rate of 0.5cm yr^{-1} estimated from radiocarbon dating and the measured frequency of discrete laminations per section seen in Table1, the laminations can be classified as varves and used as a tool to identify seasonal variability in the depositional regime of Muchalat Inlet.

Dark, organic rich laminations are associated with a high influx of TOC bound sediments transported into the inlet during periods of high run off during the winter months (Chang et al. 2013). Sediments transported into the fjord during these times are expected to be composed of a higher mass % of coarse grained particles relative to those found in the lighter laminations, which are typically indicative of a higher deposition rate of marine organic matter and finer grained sediments relative to the dark bands (Chang et al. 2013). While the mean grain size of the four sediment samples used ranged from a medium to coarse silts, samples c and d, which were taken either partially or entirely from dark laminations, had a higher mass% of sands relative to the other two samples. This is evidence that the sediments in the darker laminations

were transported and deposited during the winter. Of course, four samples isn't enough to prove this relationship. The grain size analysis procedure involves frequent transfer of materials between containers leaving room for sample material to be lost. Pipette analysis also provides a very approximate measure of % mass contribution of fine grains, and any kind of disturbance to the settling column or mis-timed sampling can result in error.

The results of $\delta^{13}C$ analysis contradict the previously mentioned results. The darker laminations had heavier $\delta^{13}C$ ratios than every adjacent light band, suggesting that the dark bands contain a significantly larger portion of marine derived carbon than the light bands **(FIGURE ?)**. One hypothesis was that C4 plants were influencing the results, but British Columbia's coast is dominated by C3 vegetation and the uncommon patch of C4 grasses wouldn't influence these results(Hay et al. 2009) Another hypothesis is that these laminations contain unusually high abundances of cool-water marine diatoms (*Fgrailariopsis pacifica*), but it seems unlikely that their biomass would have such a significant and reoccurring impact on Δ13C in an area that receives so much TOC (Nuwer and Keil 2005; Chang et al. 2013).

Another significant result of the $\delta^{13}C$ is the wide range values throughout the core (Figure 11). Values ranged from -27.1‰ to -25.22‰ in the box core and -26.7‰ to -24.97‰ in the Kasten core. I was unable to determine the cause of this, but I suspect it is due in some part non-seasonal weather patterns such as el Niño/la Niña and increases/decreases in primary productivity.

There was also a large disparity between $\delta^{13}C$ values of sediments taken from the box and Kasten cores at the same depth (Figure 11). The box core samples always had a lighter ratio than the Kasten core samples. The only difference between the ways the two sample sets were handled is the box core sediments were left at room temperature in a room with windows for

three weeks. It is hypothesized that possible contamination from photoautotrophic bacteria may have caused the change in Δ13C values.

Trace Metals

Most of the sediments tested for metals abundance were taken from samples initially chosen for grain size analysis. Grain size analysis requires a significant amount of material and the majority of samples had to be taken from adjacent laminations, so trace metal concentrations are not representative of any single deposition event. That being said, they still provide significant evidence of historical redox conditions in Muchalat inlet (Horowitz 1985; Calvert and Pedersen 1993; Chang et al. 2015).

Under sulfate-reducing conditions alone, typical of an anoxic basin cut off from deep water renewal by a sill, Ni, Cu, Zn, Cd, and Mo are typically enriched (Calvert and Pedersen 1993; Tribovillard et al. 2006). In the laminated section of the box core all four of those elements have an EF >1 and both Mo and Cd had a mean EF of over 240 with a standard deviation of ~40 (Table 3).

Enriched Molybdenum is often used as a paleoproxy for anoxic sediments, and its enrichment throughout the length of the laminated section, accompanied by the complete lack of depletions in Ni, Cu, Zn, and Cd is evidence that that section has been under anoxic conditions in the presence of H_2S (Horowitz 1985; Calvert and Pedersen 1993; Tribovillard et al. 2006) Cd extreme enrichment may be due to run off from industrial activity, possibly from mining activity or the pulp mill that operated on Gold River throughout the late 20th century (Pascaud et al. 2015).

Mn, Ba, K, and Si were all depleted throughout the entire core and Ag was only enriched in the top few cm (Table 3, Figures 6, 7, 8,9). Mn is transported upwards in its dissolved phase and

becomes insoluble when it reaches a redox boundary at 5.5cm depth. A peak in Ag at the same depth may be representative of an oxygenation event in the bottom sediments. This is supported by the fact that the sediments are homogenized, likely due to bioturbation or due to mixing from frictional forces.

Other trends, including concentration peaks just below the surface-water interface and co-varying concentrations are most likely results of redox sensitive trace metals, sulfide reduction, or the deposition of organic material.

Further studies should take use of more coring locations, preferably in the deep basin, next to the sill and outside of the sill. They should also do more metals analysis, use Pb-210 dating for higher resolution age profiles, and perform more grain size analyses on dark and light layers of sediment. These kind of studies can help monitor environmental impacts of industrial activities and act as a tool to help mitigate damages.

References

Blott, S. J., and K. Pye. 2001. Gradistat: A grain size distribution and statistics package for the analysis of unconsolidated sediments. Earth Surf. Process. Landforms **26**: 1237–1248.

Brock, F., T. Higham, P. Ditchfield, and C. B. Ramsey. 2010. Current Pretreatment Methods for AMS Radiocarbon Dating at the Oxford Radiocarbon Accelerator Unit (ORAU). Radiocarbon **52**: 103–112.

Brumsack, H. J. 2006. The trace metal content of recent organic carbon-rich sediments: Implications for Cretaceous black shale formation. Palaeogeogr. Palaeoclimatol. Palaeoecol. **232**: 344–361.

Calvert, S. ., and T. . Pedersen. 1993. Geochemistry of Recent oxic and anoxic marine sediments: Implications for the geological record. Mar. Geol. **113**: 67–88.

Chang, A. S., M. A. Bertram, T. Ivanochko, S. E. Calvert, A. Dallimore, and R. E. Thomson. 2013. Annual record of particle fluxes, geochemistry and diatoms in Effingham Inlet, British Columbia, Canada, and the impact of the 1999 La Niña event. Mar. Geol. **337**: 20–34.

Chang, A. S., L. Pichevin, T. F. Pedersen, V. Gray, and R. S. Ganeshram. 2015. New insights into productivity and redox-controlled trace element (Ag, Cd, Re, and Mo) accumulation in a 55 kyr long sediment record from Guaymas Basin, Gulf of California. Paleoceanography **30**: 77–94.

Dodimead, a. J. 1984. A review of some aspects of the physical oceanography of the continental shelf and slope waters off the west coast of Vancouver Island. Can. Manuscr. Rep. Fish. Aquat. Sci. **1773**: 309 p.

Goñi, M. a., K. C. Ruttenberg, and T. I. Eglinton. 1998. A reassessment of the sources and importance of land-derived organic matter in surface sediments from the Gulf of Mexico. Geochim. Cosmochim. Acta **62**: 3055–3075.

Hay, M. B., S. E. Calvert, R. Pienitz, A. Dallimore, R. E. Thomson, and T. R. Baumgartner. 2009. Geochemical and diatom signatures of bottom water renewal events in Effingham Inlet, British Columbia (Canada). Mar. Geol. **262**: 50–61.

Hedges, J. I. 1976. Land-derived organic matter in surface sediments from the Gulf of Mexico. Geochim. Cosmochim. Acta **40**: 1019–1029.

Hedges, J. I., and R. G. Keil. 1995. Sedimentary organic matter preservation: an assessment and speculative synthesis. Mar. Chem. **49**: 137–139.

Horowitz, a. 1985. A primer on trace metal- sediment chemistry. U.S. Geol. Surv. Water-Supply Pap. 72.

Huang, K. M., and S. Lin. 2003. Consequences and implication of heavy metal spatial variations in sediments of the Keelung River drainage basin, Taiwan. Chemosphere **53**: 1113–1121.

King, C. a. M. 1978. Geological oceanography. Mar. Geol. **28**: 293.

McCune, B., and M. J. Mefford. 2011. Multivariate Analysis of Ecological Data. Version 6.

Milliman, J. D., and J. P. M. Syvitski. 1992. Geomorphic/Tectonic Control of Sediment Discharge to the Ocean: The Importance of Small Mountainous Rivers. J. Geol. **100**: 525–544.

Nuwer, J. M., and R. G. Keil. 2005. Sedimentary organic matter geochemistry of Clayoquot Sound, Vancouver Island, British Columbia. Limnol. Oceanogr. **50**: 1119–1128.

Pickard, G. 1963. Oceanographic characteristics of inlets of Vancouver Island, British Columbia. J. Fish. Board Canada **0**.

Sachs, J. P., and D. J. Repeta. 2000. The purification of chlorins from marine particles and sediments for nitrogen and carbon isotopic analysis. Org. Geochem. **31**: 317–329.

Schropp, S. J., and H. L. Windom. 1988. a Guide To the Interpretation of Metal Concentrations in Estuarine Sediments.

Schumacher, B. a. 2002. Methods for the Determination of Total Organic Carbon in Soils and Sediments. Carbon N. Y. **32**: 25.

Tribovillard, N., T. J. Algeo, T. Lyons, and A. Riboulleau. 2006. Trace metals as paleoredox and paleoproductivity proxies: An update. Chem. Geol. **232**: 12–32.

Walsh, E. E. M., A. E. A. Ingalls, and R. G. R. Keil. 2008. Sources and transport of terrestrial organic matter in Vancouver Island fjords and the Vancouver-Washington Margin: A multiproxy approach using d 13Corg,. Limnol. … **53**: 1054–1063.

Wedepohl, K. H. 1971. Environmental influences on the chemical composition of shales and clays. Phys. Chem. Earth **8**: 305–333.

1996. Method 3050B. 1–12.

(http://www.calib.qub.ac.uk/CALIBomb/).

(http://stableisotopefacility.ucdavis.edu).